



Cite this: *Nanoscale*, 2025, **17**, 2423

## Advances in integrated power supplies for self-powered bioelectronic devices

Yu Xin,  †<sup>a,b</sup> Bin Sun, †<sup>a</sup> Yifei Kong,<sup>a</sup> Bojie Zhao,<sup>a</sup> Jiayang Chen,<sup>a,c</sup> Kui Shen <sup>b</sup> and Yamin Zhang \*<sup>a</sup>

Bioelectronic devices with medical functions have attracted widespread attention in recent years. Power supplies are crucial components in these devices, which ensure their stable operation. Biomedical devices that utilize external power supplies and extended electrical wires limit patient mobility and increase the risk of discomfort and infection. To address these issues, self-powered devices with integrated power supplies have emerged, including triboelectric nanogenerators, piezoelectric nanogenerators, thermoelectric generators, batteries, biofuel cells, solar cells, wireless power transfer, and hybrid energy systems. This mini-review highlights the recent advances in the power supplies utilized in these self-powered devices. A concluding section discusses the subsisting challenges and future perspectives in integrated power supply technologies and design and manufacturing of self-powered devices.

Received 7th November 2024,  
 Accepted 7th January 2025

DOI: 10.1039/d4nr04645e

rsc.li/nanoscale

### 1. Introduction

With the development of modern biomedical technologies, bioelectronic devices have become powerful solutions for healthy,

comfortable and high-quality life.<sup>1–3</sup> In such devices, the power supply is one of the most important parts. Recently, various light-weight power supplies have been designed for self-powered wearable and implantable bioelectronics, which eliminate the need for external power supplies and extended electrical wires being used in conventional biomedical devices.<sup>4–15</sup> However, the trend towards small-volume and light-weight power supplies inevitably results in insufficient energy and frequent replacements. Simply increasing the energy densities of these power supplies may cause safety concerns.<sup>16,17</sup> Consequently, the development of self-powered bioelectronic devices with reliable and stable integrated power supplies is highly desired.

<sup>a</sup>Department of Chemical and Biomolecular Engineering, College of Design and Engineering, National University of Singapore, 117585, Singapore.

E-mail: ymzhang@nus.edu.sg

<sup>b</sup>School of Chemistry and Chemical Engineering, South China University of Technology, Guangzhou, 510640, China

<sup>c</sup>College of Chemistry, Nankai University, Tianjin, 300071, China

†These authors contributed equally to this work.



**Yu Xin**

Yu Xin is a joint Ph.D. student under Prof. Yamin Zhang's supervision in the Department of Chemical & Biomolecular Engineering, National University of Singapore, Singapore. He is also a Ph.D. candidate under Prof. Kui Shen's supervision in the School of Chemistry & Chemical Engineering, South China University of Technology, China. He received his B.Eng. degree in 2019 and M.Eng. degree in 2021 from Hainan

University and Sun Yat-sen University, respectively. His current research focuses on the design of new electrochemical devices for human healthcare and electrocatalytic energy conversion.



**Bin Sun**

Bin Sun is a Ph.D. candidate under Prof. Yamin Zhang's supervision in the Department of Chemical & Biomolecular Engineering, National University of Singapore, Singapore. He received his B.Sc. degree in 2024 from Zhejiang University, China. His current research focuses on the application of electrochemistry in healthcare.



The integration of power supplies into bioelectronic devices has sparked an innovative concept of self-powered bioelectronics.<sup>18–20</sup> Such self-powered devices contain various types of power supplies, including triboelectric nanogenerators (TENGs),<sup>21–23</sup> piezoelectric nanogenerators (PENGs),<sup>24–26</sup> thermo-electric generators (TEGs),<sup>27,28</sup> batteries,<sup>29,30</sup> biofuel cells (BFCs),<sup>31–35</sup> solar cells (SCs),<sup>36</sup> and wireless power transfer (WPT) systems.<sup>37–39</sup> However, it is still of great difficulty to seamlessly integrate these self-powered technologies into smart devices, which requires cutting-edge design concepts and advanced microfabrication strategies. The rapid growth of research outputs in these areas poses the need for review articles that summarize recent advances.<sup>40–48</sup> For example, a self-powered intracardiac pacemaker based on triboelectrification and electrostatic induction was put forward for the treatment of arrhythmia.<sup>44</sup> A self-powered, light-controlled and wirelessly programmed drug delivery device was designed for the programmed release of drugs.<sup>29</sup>

In this mini-review, we start with a brief description on the fundamentals of self-powered devices. After that, we present the current progress of various self-powered wearable and implantable devices integrated with power supplies including TENGs, PENGs, TEGs, BFCs, batteries, SCs, WPT systems and their hybrid power sources. Finally, the subsisting challenges and future perspectives of self-powered bioelectronic devices are also discussed.

## 2. Fundamentals of self-powered devices

The term “self-powered” means that the device has its own power supply or propelling force according to the Merriam-Webster dictionary.<sup>49</sup> Fig. 1 presents some typical examples of

self-powered bioelectronic devices that utilize TENGs, PENGs, TEGs, BFCs, batteries, SCs as power supplies.<sup>29,36,44,50–52</sup> Electric generators (TENGs, PENGs and TEGs) obtain energy from external skin motion, internal body–organ movement, and temperature difference (Fig. 1a, b and c). They exhibit smaller size, better biocompatibility and higher sustainability compared with the traditional external power supplies, which makes them more suitable to be integrated into self-powered devices for diagnostic and therapeutic applications.

In addition, batteries are one kind of power supply being widely used in biomedical devices which convert chemical energy into electricity. Though Li-ion batteries are the mostly used type, this article focuses on advanced biocompatible battery technologies, which utilize biocompatible or bioresorbable battery materials and components (Fig. 1d). Biofluid-activated BFCs convert biochemical energy into electrical energy with the assistance of biocatalysts (Fig. 1e). Glucose and lactate which are widely distributed in human biofluids (*i.e.*, sweat, tears, gastrointestinal fluid, urine, *etc.*) can act as “bio-fuels” and be oxidized by oxygen to generate electric power. They have low energy density and are typically safe even short-circuit occurs. SCs can provide sustainable, clean, and renewable energy, demonstrating significant potential in self-powered bioelectronic devices (Fig. 1f). SC-based devices not only convert sunlight directly into electric energy, but also store the generated energy to power the devices. Besides, the WPT technology in bioelectronic devices usually use electromagnetic field induction to transmit power, in which the transmitter coil generates time-varying electromagnetic waves in the radio wave frequency (RF) range which can induce a current in the receiver coil. Given the different operating conditions of the power supplies mentioned above, they need to be contextualized and thus integrated into different medical bioelectronic devices. In some cases, these power supplies can



**Kui Shen**

*Kui Shen is a full professor in the School of Chemistry & Chemical Engineering, South China University of Technology, China. He received his Ph.D. degree from Tsinghua University in 2014 and performed his post-doctoral research work at South China University of Technology from 2014 to 2016. After that he worked as an associate research fellow at South China University of Technology from 2016 to 2018. His current research*

*focuses on the design and synthesis of new porous materials and their applications in heterogeneous catalysis, electrocatalysis and photocatalysis.*



**Yamin Zhang**

*Yamin Zhang is an assistant professor under Presidential Young Professorship at the Department of Chemical & Biomolecular Engineering in the National University of Singapore (NUS). She was a postdoctoral fellow (2021–2024) in Prof. John A. Rogers's group at Northwestern University. She received her Ph.D. degree from Georgia Institute of Technology in 2020 under the supervision of Prof. Nian Liu. Her research focuses on advancing*

*electrochemical strategies for next-generation medical devices and sustainable energy solutions. She is a recipient of several grants/awards, including the AHA Early Faculty Independence Award (2023), MIT ChemE Rising Stars (2022), the Best PhD Thesis Award at Georgia Tech (2020), etc.*





**Fig. 1** Examples of some typical self-powered biomedical devices and integrated power supplies. (a) The internal perspective structure and mechanism of a TENG in an intracardiac pacemaker. Adapted from ref. 44 with permission from Nature Springer, Copyright 2024. (b) The photograph and mechanism of a PENG in a microneedle drug delivery system. Adapted from ref. 50 with permission from John Wiley and Sons, Copyright 2021. (c) The photograph and mechanism of a TEG in a wound healing device. Adapted from ref. 49 with permission from John Wiley and Sons, Copyright 2024. (d) The photograph and mechanism of galvanic cells in a light-controlled drug delivery system. Adapted from ref. 29 with permission from the National Academy of Sciences, Copyright 2023. (e) The photograph and mechanism of a BFC in an ascorbic acid-assisted sweat patch. Adapted from ref. 51 with permission from John Wiley and Sons, Copyright 2024. (f) The photograph and mechanism of an SC in a wearable sweat sensor. Adapted from ref. 36 with permission from Nature Springer, Copyright 2023.



be integrated together to form hybrid power supplies. This may become the future trend for long-term continuous operation.

### 3. Integrated power supplies for self-powered devices

The emerging power supplies (*e.g.*, TENGs, PENGs, TEGs, batteries, SCs) convert mechanical, thermal, electrochemical, biofuel and solar energies into electric energy. TENGs and PENGs are representative power supplies which can utilize the mechanical energy from human motions. TEGs utilize the temperature difference between the human body and the environment to convert thermal energy into electric energy. Batteries, a package of one or more galvanic cells, generate electricity from chemical energy. BFCs utilize biofluids (*e.g.*, sweat) and convert bioenergy into electric energy, in which the biofluids, oxygen and enzymes act as the biofuel, oxidant and biocatalysts, respectively. SCs convert solar energy into electrical energy when exposed to sunlight. The WPT technology can achieve electromagnetic energy transmission without physical connectors by controlling the electromagnetic field. Hybrid energy systems include any combination of the above-mentioned power supplies.

#### 3.1. Triboelectric nanogenerators

Based on the effects of contact electrification and electrostatic induction,<sup>53,54</sup> TENGs can harvest mechanical energy and convert it to electric energy. Firstly, electrons between two different materials can spontaneously transfer through contact electrification. After separating them, these two materials become electrically charged. In order to maintain the electrostatic equilibrium between them, electrons flow in the external circuit. Therefore, TENGs equipped with self-powered devices can supply stable alternating current (AC). Recently, a flexible transparent electrode (FTE) composed of Mxene nanosheets, alginate and glycerol was prepared.<sup>55</sup> Its triboelectric potentials with various clothing fabrics, including polytetrafluoroethylene (PTFE) fiberglass, polyester fiber, acetate fiber tropical suiting, knitting wool, imitation silk, *etc.*, were evaluated. These commonly used fabrics exhibited high-output voltages. The assembled TENG composed of an FTE and a PTFE not only drives the release of antibacterial drugs, but also provides electrical stimulation for accelerated wound healing. Due to the contact electrification principle, FTE and PTFE surfaces generate positive and negative charges, respectively (Fig. 2a). As the PTFE and FTE are separate, the positive charges generated from the FTE can be transferred to silver fabric and thus form current simultaneously. When the PTFE re-approaches the FTE, the current in an opposite direction can be formed, which provides electrical stimulation to the wound tissue for cell migration, cell proliferation, and collagen deposition.

Recently, a TENG-powered dissolvable microneedle patch for deep-seated melanoma therapeutics was reported,<sup>56</sup> in which the microneedle is composed of water-soluble polymers

and therapeutic drugs diffuse through the epidermis *via* iontophoresis driven by the TENG. The TENG, composed of silicone rubber and a conductive textile, outputs an AC and a short-circuit current ( $I_{sc}$ ) of 54  $\mu$ A. By converting the generated AC to direct current (DC) through a power management system (PMS),<sup>57</sup> the output current reaches 1.5 mA, which is enough to drive the drug delivery in the iontophoresis process. In addition to facilitating drug penetration for deep-seated melanoma therapeutics,<sup>56</sup> inflammatory skin disorders,<sup>58</sup> and intervertebral disc degeneration repair,<sup>59</sup> the TENG-powered microneedle patch can also promote tendinopathy treatment through transcutaneous electrical stimulation.<sup>60</sup> The pulsed electric output generated directly from TENGs can improve the pharmacodynamics of epidermal growth factor. Besides, a flexible plate-based TENG with polyamide (nylon 6) and poly(vinylidene fluoride-trifluoroethylene) (PVDF-TrFE) films was also used as the power supply of an electrical patch for stimulating collagen regeneration in the tendon.<sup>61</sup> The TENG patch (5 mm  $\times$  5 mm) affixed to the leg of a rat exhibited an output voltage of 5–8 V when the rat moved. Although the patch doesn't contain microneedle structure, the electric field generated from this is also able to penetrate through the skin into a depth of hundreds of microns ( $>150$   $\mu$ m) according to the results of multiphysics COMSOL simulation.

In addition to wearable TENG-based devices, implantable TENG-powered devices made of biocompatible and biodegradable materials have also caught the attention of researchers. For example, the synthesized biodegradable elastomers (polyurethane and poly(lactide-*co*- $\epsilon$ -caprolactone)) and metal oxide nanoparticles (ZnO and MoO<sub>3</sub>) yielded stretchable, dissolvable triboelectric nanocomposites.<sup>13</sup> The combination of metal oxide nanoparticles with polymer matrices not only enhances triboelectric performance, but also biodegradability and deformability. Besides, a fully implantable, bioresorbable, and ultra-flexible TENG was produced for bone regeneration.<sup>62</sup> This TENG-powered device delivers a consistent output of at least 4.5 V, which can ensure sufficient electrical stimulation for (i) hematoma formation and the inflammatory phase, (ii) callus generation, (iii) primary bone formation, and (iv) bone remodeling (Fig. 2b). Due to the electroactive properties of the myocardium, the PENG-powered conductive cardiac patch was prepared to rebuild the electroactive microenvironment for the infarcted myocardium by electrical stimulations.<sup>63</sup> In this cardiac patch, a polydopamine (PDA)-modified reduced graphene oxide (rGO) membrane and a PVDF film were employed as the electrode and triboelectric layer, respectively (Fig. 2c). Such a cardiac patch exhibited a remarkable reparative effect on the infarcted heart in minipig models. Besides, TENG-powered electrostimulators show great potential in peripheral nerve regeneration.<sup>64</sup> As shown in Fig. 2d, a bioresorbable neurostimulator with an acoustically triggerable transient TENG (ACT-TENG) and a bioresorbable cuff electrode was prepared. The cuff electrode composed of poly(3-hydroxybutyrate-*co*-3-hydroxyvalerate) (PHBV) membranes and Mg electrodes can deliver the AC electrical impulses (20 kHz, 7.76 V) generated from ACT-TENG to the targeted site of the sciatic nerve. Such a





**Fig. 2** Exemplary works of TENGs. (a) Working mechanism of the self-powered TENG microneedle system for wound dressing. Adapted from ref. 55 with permission from Elsevier, Copyright 2024. (b) Schematic illustration of the TENG-powered electrical stimulator for bone regeneration. Adapted from ref. 62 with permission from the National Academy of Sciences, Copyright 2021. (c) TENG-powered cardiac patch for repairing infarcted myocardium. Adapted from ref. 63 with permission from Nature Springer, Copyright 2024. (d) TENG-powered bioresorbable neurostimulator. Adapted from ref. 64 with permission from Nature Springer, Copyright 2023.

neurostimulator has shown distinct improvements for both compression peripheral nerve injury and hereditary peripheral neuropathy (Charcot–Marie–Tooth disease type 1 A, CMT1A).

### 3.2. Piezoelectric nanogenerators

PENGs mainly harvest mechanical energy and convert it to electrical energy through the piezoelectric effect of various piezoelectric materials such as zinc oxide (ZnO), poly(vinylidene fluoride) (PVDF), lead zirconate titanate (PZT), and barium titanate (BaTiO<sub>3</sub>).<sup>24</sup> When a force is applied to the piezoelectric material, the increase of polarization charge density generates an electric field with equivalent negative and positive charges on both sides of the piezoelectric layer, and if an external circuit is connected with both sides of the piezoelectric material, a current can be formed in the circuit. Due to its excellent flexibility and high biocompatibility, PVDF has been widely used as a piezoelectric layer in the fabrication of wearable PENGs. Fig. 3a shows a typical structure of a wearable PENG drug delivery patch. In this design, a PVDF film serves as the piezoelectric layer, polyethylene terephthalate (PET) serves as the encapsulation layer, an Ag film serves as the electrode layer, and a Kapton film serves as the substrate layer.<sup>50</sup>

Cu tape on the Ag electrode layers was connected with Cu wires to output the current generated from the PENG. As an external force was applied and removed, a continuous AC in the external circuit can be generated (Fig. 3b). Besides, an arched shape memory PENG composed of PET, PVDF, Ag, and Kapton was also used to power an implanted therapeutic device.<sup>65</sup> The short-circuit current generated from the arched PENG (20  $\mu$ A) is twice as large as that of the flat PENG (8.2  $\mu$ A) with lightly tapping, which indicates that the arched structure can increase the electrical output by enhancing the stress and strain of the PENG.

Recently, a self-powered PVDF-based PENG was integrated with a microneedle module to achieve controllable drug delivery.<sup>66</sup> In order to enhance the piezoelectric properties of the PVDF layer, a piezoelectric composite fiber film composed of carbon nanotubes (CNTs) and PVDF was prepared by the electrostatic spinning method. The PVDF/CNT layer not only exhibits flexible mechanical characteristics (stretch up to 125%), but also exhibits an open circuit voltage of 0.88 V under a finger press pressure of 0.742 kPa, making it suitable to drive a microneedle drug (sodium nitroprusside) delivery system. During the drug releasing process, the release rate is



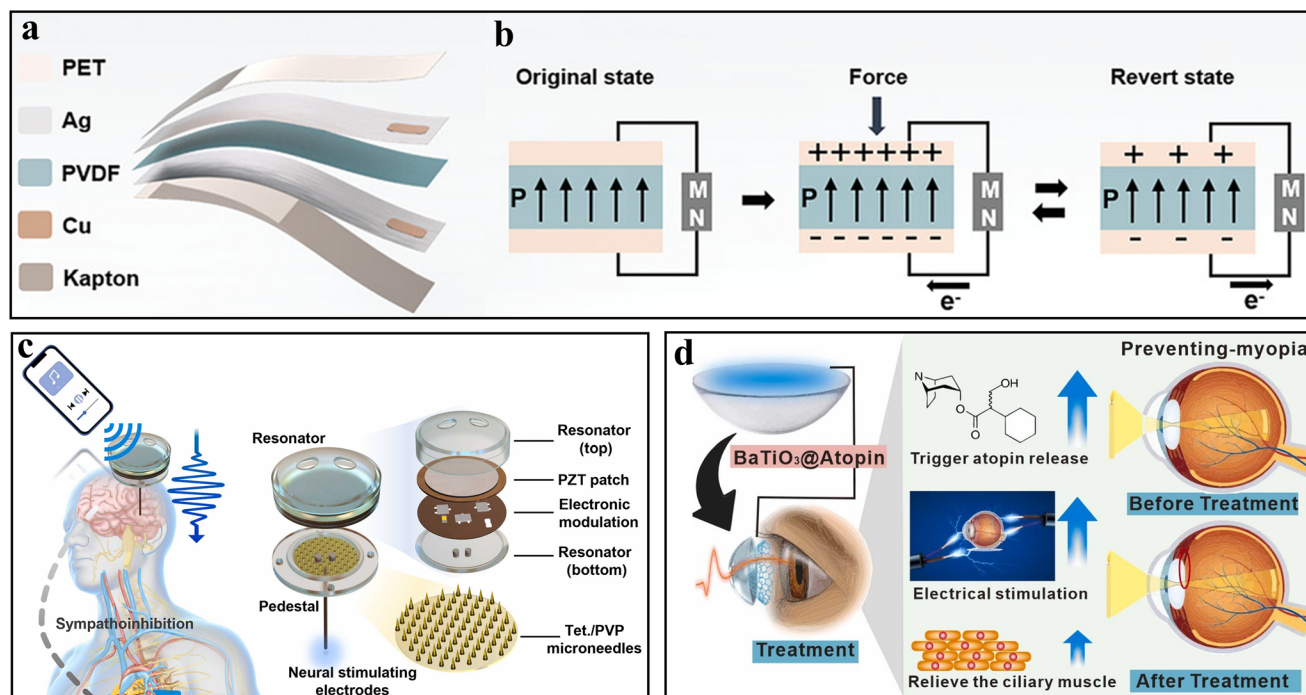


**Fig. 3** Exemplary works of PENGs. (a) Schematic illustration and (b) working mechanism of a PVDF-based PENG. Adapted from ref. 50 with permission from John Wiley and Sons, Copyright 2021. (c) Schematic illustration and working mechanism of a PZT-based PENG therapeutics device. Adapted from ref. 67 with permission from Elsevier, Copyright 2023. (d) BaTiO<sub>3</sub>-based PENG contact lenses with blink-activated drug release. Adapted from ref. 68 with permission from Elsevier, Copyright 2024.

always positively correlated with both pressing frequency and pressure. In addition to finger pressing, acoustic energy can also activate the piezoelectric transducer (as resonator) by program-specific audio signals. A brain probe with piezoelectric transducer driven by acoustic waves was reported.<sup>67</sup> The PZT-based piezoelectric transducer was installed in a Helmholtz resonant cavity, and it can be regarded as a resonator to convert the acoustic wave mechanical energy to electrical energy based on the piezoelectric effect (Fig. 3c). By combining such a PENG with brain stimulating electrodes, this brain probe device can achieve an electrical stimulation regulation of blood pressure without external power supplies.

A suitable rhythmic cadence of blinks can also activate the contact lens-like PENG biomedical devices placed on the eye. For example, a drug-coated BaTiO<sub>3</sub>-based PENG, designed to be carried on contact lenses, was reported (Fig. 3d).<sup>68</sup> Through the Mitsunobu reaction, atropine drugs can be covalently tethered onto the BaTiO<sub>3</sub> nanoparticles. The embedded BaTiO<sub>3</sub>-based PENG with atropine can generate a stable output voltage of about 10 V when blinking eyes 17 times per minute. This pulsed electrical stimulation causes reversible deformation and redox state changes in BaTiO<sub>3</sub>, triggering the release of therapeutic atropine from the BaTiO<sub>3</sub>@Atropine nanoparticles.

### 3.3. Thermoelectric generators

In addition to the above typical TENGs and PENG, TEGs can also act as the power supply in self-powered devices due to the thermoelectric properties of various thermoelectric materials

(such as Ag<sub>2</sub>Se and Bi<sub>2</sub>Te<sub>3</sub>). According to the Seebeck effect, a temperature difference between the connected n-type and p-type legs can generate a voltage drop between them.<sup>69</sup> Thus, the TEGs integrated with wearable devices can produce a few microvolts of electricity from the temperature difference between the human body and the environment. For example, p-type and n-type Bi<sub>2</sub>Te<sub>3</sub>-based thermoelectric powders, known for their excellent thermoelectric performance at room temperature, can be used to prepare bead-like ternary hierarchically coaxial TE strings (THC-TES) for 3D multilayer textile (Fig. 4a).<sup>70</sup> Such textile not only exhibits an output power density of 0.58 W m<sup>-2</sup> (temperature difference  $\Delta T = 25$  K), but also has excellent mechanical stability with a bending radius of  $\sim 2$  mm and even can be knotted. This PEG-powered textile worn on the forearm ( $\Delta T = 16$  K) can continuously power the electronic devices for human health monitoring. Besides, the Bi<sub>2</sub>Te<sub>3</sub>-based compounds can be used to design a PEG-powered wound healing device, in which Bi<sub>2</sub>Te<sub>3</sub> and Bi<sub>0.5</sub>Sb<sub>1.5</sub>Te<sub>3</sub> are regarded as the n-type and p-type legs, respectively.<sup>52</sup> This flexible device covered with a biocompatible polyimide layer can efficiently utilize body's self-heat to generate electricity. This process could also accelerate wound healing in turn by electrical stimulation in a rat model (Fig. 4b). Compared to other external large power generation system, such kind of TEG-powered wound healing device is able to provide safe electrical stimulation (small voltage/current) without an additional amplifier, making itself more suitable for flexible and wearable self-powered biomedical devices.





**Fig. 4** Exemplary works of TEGs. (a) Diagrams and corresponding knotting/bending images of the THC-TES with vertical arrangement of p-type and n-type segments. Adapted from ref. 70 with permission from the Royal Society of Chemistry, Copyright 2022. (b) Schematic illustration of TEG-powered electrical stimulation for wound healing. Adapted from ref. 52 with permission from John Wiley and Sons, Copyright 2024.

### 3.4. Batteries

Batteries, mainly Li-ion batteries, are power supplies being widely used in biomedical devices, however, with safety concerns. Recent efforts are on developing lightweight and flexible biocompatible and/or bioresorbable batteries capable of being integrated into self-powered wearable and implantable devices.<sup>71</sup> The battery is a package of one or more galvanic cells. In some cases, the battery itself serves as both the power supply and the functional part for biomedical applications (e.g., drug release,<sup>72</sup> electrotherapeutics,<sup>73</sup> and sensors<sup>74,75</sup>), which reduces the need for complex circuits and electronic components. For example, a self-powered gate valve device was designed for controlled drug release, where Mg metal anodes act as the gates of drug reservoirs, which pairs with a Fe cathode to form galvanic cells.<sup>29</sup> The biofluid serves as the electrolyte. As shown in the exploded view illustration (Fig. 5a), the self-powered device includes three bioresorbable Mg anodes (gates) and an Fe cathode. The gates seal three drug reservoirs. The cathode and anodes are interconnected by a set of three phototransistors and optical filters. Illuminating the phototransistor with light of a specified wavelength range reduces its resistance, discharges the corresponding galvanic cell, corrodes the Mg gate, and thus allows drug release (Fig. 5b). Such a self-powered gate valve device can achieve controllable release of one specific kind or multiple kinds of drugs by illumination with monochromatic light or multicolor light. In addition, a cathodic cytocompatible viologen-based hydrogel can also act as the drug reservoir (Fig. 5c).<sup>72</sup> During



**Fig. 5** Exemplary works of batteries. (a) Exploded view illustration of an implantable self-powered drug delivery device. (b) Release of drugs from the gate valve due to light-controlled self-powered anodic Mg corrosion. Adapted from ref. 29 with permission from the National Academy of Sciences, Copyright 2023. (c) Schematic diagram and corresponding photographs of a wearable Mg battery-powered drug release patch. (d) Mechanism of Dex drug release from a cathodic P(AM-co-SV) hydrogel. Adapted from ref. 72 with permission from Nature Springer, Copyright 2023.



discharge, the electrostatic interaction between the hydrogel and the anionic drug dexamethasone (Dex) decreases and thus leads to the release of the Dex drug (Fig. 5d). The release rate of Dex can be controlled by tuning the resistance value of external resistors. This cell supplies a high energy density of  $3.57 \text{ mW h cm}^{-2}$ , which is enough to drive the iontophoresis to achieve potential-controlled drug release.

In addition to drug delivery, galvanic cell-based self-powered devices can also be used for electrical stimulation. For example, an Mg–FeMn battery with Mg as the anode and FeMn alloy as the cathode allows continuous electrical stimulation for neurons axonal outgrowth.<sup>73</sup> The anodic reaction is Mg oxidation ( $\text{Mg} \rightarrow \text{Mg}^{2+} + 2\text{e}^-$ ), while the cathodic reactions include oxygen reduction ( $\text{O}_2 + 2\text{H}_2\text{O} + 4\text{e}^- \rightarrow 4\text{OH}^-$ ) and hydrogen evolution ( $2\text{H}^+ + 2\text{e}^- \rightarrow \text{H}_2$ ). The average open circuit voltage of the Mg–FeMn cell can remain up to 0.984 V after 24 h operation. Besides, a wearable sweat-activated self-powered sensor was designed. This device has equipped two Mg batteries as power supplies, in which Mg, Ag/AgCl and sweat serve as the anode, cathode and electrolyte, respectively. In a sweat-free environment, the device remains in an open circuit, which is safe for the human body with no risk of leakage or self-discharge. During the perspiration process, the device is activated to monitor the heart rate, sweat pH and  $\text{Cl}^-$  concentration.<sup>75</sup>

### 3.5. Biofuel cells

BFCs utilize biofluids as the biofuel to generate electricity, which couples the anodic biofuel oxidation reaction (BOR) with the cathodic oxygen reduction reaction (ORR). As one of the most common types of BFCs, enzyme fuel cells (EBFCs) rely on the cell aerobic metabolism to consume oxidizable fuel and generate electrical power using biocatalysts including anodic glucose oxidase (GOx), lactate oxidase (LOx), and alcohol oxidase (AOx) for BOR, and cathodic laccase and bilirubin oxidase (BOD) for ORR. However, the existence of cell membranes has limited the power densities of MBFCs by slowing down the electron transfer from the enzyme to the anode surface. Thus, directly loading these enzyme biocatalysts on the surface of electrodes can surpass this output power limit and facilitate the application of EBFCs in bioelectronic devices. Combining GOx and BOD with carbon nanotube (CNT)-coated Ni foam electrodes forms the enzyme-loaded anode and cathode of a glucose-based EBFC in the gastrointestinal environment, respectively. The EBFC powers the glucose sensor (Fig. 6a).<sup>76</sup> Tetrathiafulvalene-7,7,8,8-tetracyanoquinodiamethane (TTF-TCNQ) and 2,2'-azino-bis(3-ethylbenzothiazoline-6-sulfonic acid) ( $\text{ABTS}^{2-}$ ) mediators can effectively promote electron transfer on the anode and cathode, respectively. This self-powered battery-free device generates a power of more than  $0.4 \mu\text{W}$  even in a very low glucose concentration environment, which can activate the electronic circuitry for glucose concentration signal transmission.

Recently, anti-biofouling and flexible fiber EBFCs with intrinsic biocompatible CNT-modified fiber electrodes have shown great potential in the development of implantable

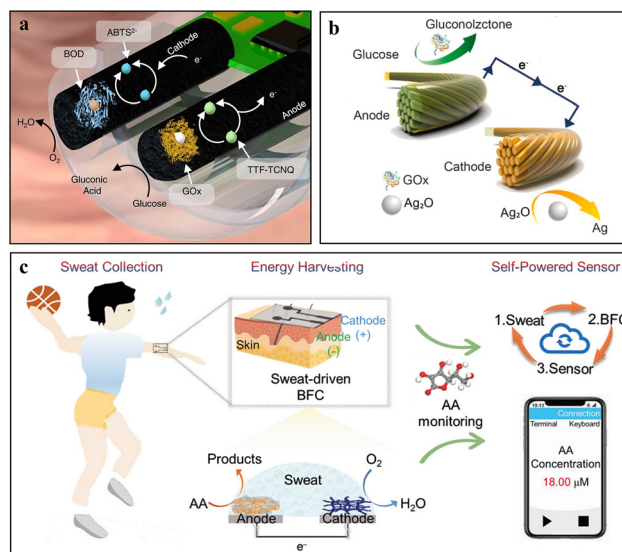


**Fig. 6** Exemplary works of BFCs. (a) Schematic illustration of a glucose BFC-powered capsule-shaped sensor in the small intestine. Adapted from ref. 76 with permission from Nature Springer, Copyright 2022. (b) Schematic illustration of a glucose BFC-powered biosensing suture. Adapted from ref. 78 with permission from Elsevier, Copyright 2024. (c) Schematic illustration of an ascorbic acid BFC-powered sweat sensing platform. Adapted from ref. 51 with permission from John Wiley and Sons, Copyright 2024.

medical devices. However, the low concentration of oxygen in the *in vivo* environment is one of the major limits for the power output of EBFCs.<sup>77</sup> Accordingly, glucose-based EBFC biosensing sutures have been put forward, in which tetrathiafulvalene/GOx-modified carbon fiber and Ag<sub>2</sub>O/CNT-modified carbon fiber serve as the anode and cathode, respectively (Fig. 6b).<sup>78</sup> The sutures remain partially outside the body and thus access the atmosphere with a higher oxygen concentration compared to the *in vivo* environment. Besides, wearable devices with EBFCs (exposed to air) utilize epidermal biomarkers in sweat (*e.g.*, glucose, lactate, and ascorbic acid) to harvest bioenergy, which in turn power the sensors for biomarkers. For example, a lactic acid biofuel cell was developed by integrating a lactate oxidase (LOx)-loaded anode and a Pt–Co nanoparticle-loaded cathode.<sup>79</sup> This device achieves an excellent power density of  $3.5 \text{ mW cm}^{-2}$  in untreated human sweat and remains stable for more than 60 hours with continuous working. Recently, an ascorbic acid-based BFC platform with Au/reduced graphene oxide (Au-rGO) dual hydrogels as the anode and Pt–Cu hydrogels as the cathode was reported (Fig. 6c).<sup>51</sup> Although the ascorbic acid concentration is relatively low in sweat, the as-prepared device exhibits a maximum power density of  $35 \mu\text{W cm}^{-2}$  in the air equilibrated PBS solution containing 0.5 mM ascorbic acid. Given the diversity of biomarkers in human sweat, some exogenous metabolites in sweat such as ethanol can be generated in large quantities after alcohol drinking, a flexible wearable epidermal microfluidic ethanol/oxygen biofuel cell was prepared to collect, transmit, store and utilize fresh human sweat in real time through



a designed epidermal microfluidic module.<sup>80</sup> This design expands the biofluid in EBFCs from endogenous substances (glucose, lactate, and ascorbic acid) to exogenous metabolites (ethanol). It opens more possibilities for the applications of wearable flexible sensors such as drink-drive testing.

Microbial fuel cells (MFCs) have been widely explored besides EBFCs, which mainly utilize bacterial metabolism to convert biochemical energy in biofluids (*e.g.*, sweat) into electrical energy. In addition to the bacteria from the natural environment such as *Shewanella oneidensis* MR1, the bacteria that exist on human skin can also act as biocatalysts to “eat” sweat by metabolism effects. Due to the bacterial electrogenicity of three skin bacteria (*Staphylococcus epidermidis*, *Staphylococcus capitis*, *Micrococcus luteus*) and one ammonia-oxidizing bacteria (*Nitrosomonas europaea*), a flexible skin-mountable MFC-powered e-skin was designed.<sup>81</sup> In addition, incorporating the spores of *Bacillus subtilis* into MFCs can also promote sweat secretion and generate electrical power. The maximum power density can remain 24  $\mu\text{W cm}^{-2}$  even after working for 48 h.<sup>82</sup> Given the extensive variety of microbes living in symbiosis with the human body, it is promising to integrate bacteria that generate electricity into the fabrication of biomedical devices for health monitoring and healthcare applications.

### 3.6. Solar cells

As a renewable energy resource, light-activated SCs harvest energy from natural sunlight to power bioelectronic devices. The typical photovoltaic technologies based on silicon have limited the application in wearable devices due to the fragile and rigid characteristics of silicon. Recently, some flexible SC-integrated devices have been reported including perovskite SCs and organic SCs.<sup>83</sup> Thanks to the flexibility of organic materials, a flexible photonic skin consisting of solar cells, polymer light-emitting diodes (PLEDs) and organic photo-

detectors was designed as a self-powered device for photo-plethysmogram monitoring. In this system, the PLEDs can retain 70% of the initial brightness in such an SC-powered device after working for 11.3 h. Recently, a flexible perovskite SC-powered sweat sensor for sweat analysis under sunlight or indoor light was put forward by Gao's group (Fig. 7a).<sup>36</sup> Such a device has a flexible printed circuit board (FPSC), a FPSC power unit, and a microfluidic sensor patch, in which the 2D FPSC with p-i-n architecture with  $(\text{MBA})_2(\text{Cs}_{0.12}\text{MA}_{0.88})_6\text{Pb}_7(\text{I}_x\text{Cl}_{1-x})_{22}$  as the perovskite absorber layer play a key role for power supply (Fig. 7b). The power conversion efficiency (PCE) of this sweat sensor can reach 14.00% and 29.64% under air mass global 1.5 (AM1.5G) sunlight and 600 lx indoor LED light, respectively, which shows its potential for outdoor and indoor applications. Similarly, a novel sandwich-structured photovoltaic microcurrent hydrogel dressing (PMH dressing) was also successfully designed for facilitating wound healing. Flexible organic photovoltaic (OPV) cells integrated with the hydrogel dressing can provide suitable electrical stimulation for healing infected diabetic wounds.<sup>15</sup>

### 3.7. Wireless power transfer

The WPT technology can harness environmental energy sources like radio frequency (RF) signals, ultrasound and an ambient magnetic field to support device functions. RF power transmission is achieved by electromagnetic field induction, in which the transmitter coil generates time-varying electromagnetic waves in the RF range which can induce a current in the receiver coil of bioelectronic devices. The RF WPT technology can be directly used to power implantable bioelectronic devices such as cardiac pacemakers and nerve stimulators.<sup>37–39</sup> For example, a bioresorbable pacemaker module composed of a receiver (Rx) Mo coil, a pair of stretchable Mo interconnects, and a stimulation electrode was prepared (Fig. 8a).<sup>37–39</sup> By



Fig. 7 Exemplary works of SCs. (a) Working mechanism and (b) exploded 3D schematic illustration of a SC-powered sweat sensor. Adapted from ref. 36 with permission from Nature Springer, Copyright 2023.





**Fig. 8** Exemplary works of WPT. (a) Exploded view of a flexible wireless transfer-powered intracardiac pacemaker (b). Schematic illustration of an autonomous and wireless pacing therapy system. Adapted from ref. 37 with permission from the American Association for the Advancement of Science, Copyright 2022. (c) Schematic illustration of a wireless transfer-powered electrical stimulator for nerve regeneration. Adapted from ref. 38 with permission from John Wiley and Sons, Copyright 2023.

applying AC current to the transmission coil *in vitro*, the current in the Rx coil can be induced wirelessly, which can be further converted to a DC output by the rectifier diode for cardiac pacing (Fig. 8b). Similarly, a self-assembled microtubular electronics was also prepared for intravascular implantation.<sup>37–39</sup> The RF was also used to transfer energy to the microtubular pacemaker for electrical stimulation, eliminating the need for an energy storage unit in implanted bioelectronic devices. In addition, a nerve stimulator equipped with a biodegradable conductive nerve conduit also can be powered by RF WPT technology (Fig. 8c).<sup>37–39</sup> Such controlled wireless electrical stimulation can promote the regeneration of long nerve defects.

However, the transferred energy through high-frequency RF signals (>10 000 Hz) attenuates rapidly in bio-tissues, which has made power transmission of such implantable bioelectronic devices more difficult in deep tissues. Therefore, magneto-electric (ME) harvesters with a low working frequency (<100 Hz) are more suitable for powering implantable devices in the deep tissues because such magnetic fields are not easily absorbed by biological tissues. Recently, an ultra-low frequency magnetic energy focusing methodology was reported.<sup>84</sup> A portable external magnetic energy transmitter (EMET) can generate a low-frequency magnetic field (<50 Hz) to drive the

implantable magnetism internally focusing core (MIFC) and thus generate an internal magnetic field. By controlling the EMET, the implantable MIFC in the device can generate a changing magnetic flux and induce an electromotive force. Such an implantable device under thick tissues (~20 cm) can be powered through a low-frequency ME method with a transferred power of 4–15 mW.

These above sustainable power solutions shed light on the internet of things (IoT)-enabled bioelectronic devices, reducing dependence on batteries and supporting continuous low-power operation.

### 3.8. Hybrid energy systems

Hybrid systems combining different energy generation and storage technologies represent a pivotal area of research for self-powered bioelectronic devices. Although the widely recognized TENGs can generate high voltage, the low output current has limited their biomedical applications. To address this challenge, researchers have proposed combining TENGs with other types of power supplies to supply energy from multiple sources. Among these, PENGs with similar output characteristics, resistances, and working frequency ranges to TENGs can be regarded as the best candidates in the fabrication of hybrid triboelectric–piezoelectric nanogenerators (TPENGs).<sup>85</sup> For



instance, by using the co-electrospinning method, single-layer binary fiber nanocomposite membranes (DPCPC<sub>x</sub>-SBFNMs) composed of CNTs/PVDF and CNTs/polyacrylonitrile (PAN) can be prepared (Fig. 9a). Such a DPCPC<sub>0.5</sub>-SBFNM-based TPENG exhibited excellent electrical output (187 V, 8.0  $\mu\text{A}$ , and 1.52  $\text{W m}^{-2}$ ), which can be integrated with a piezoelectric sensor and accurately senses human movement. Besides, a flexible poly(dimethylsiloxane) (PDMS) film embedded with electrospun PVDF nanofibers can also be used to prepare a sandwich-structured hybrid TPENG.<sup>86</sup> Under an external force of 10N, such a TPENG can generate a maximum power density of 286  $\text{mW m}^{-2}$ .

Furthermore, TENGs can continuously generate thermal energy during human movement. This character also offers an attractive method to further enhance energy recovery efficiency when a TENG was combined with a TEG as a hybrid energy system. As shown in Fig. 9b, using a liquid-phase aluminum coating technique, a hybrid harvester with three layers containing a bottom aluminum-coated heat transport fabric, a heat blocking fabric with commercial thermoelectric devices (TED) and a top aluminum-coated heat transport fabric was fabricated.<sup>87</sup> The aluminum-coated fabric in such a hybrid harvester serves as a triboelectric electrode and heat-transport

layer due to its high electrical and thermal conductivity, respectively. With the assistance of a customized transforming system, such a device integrated on human clothes generates an output voltage of 3 V within 240 seconds, with an average power density of 8.25  $\text{mW m}^{-2}$ . Accordingly, such TENG/TEG hybrid power supply has the potential to alleviate the charging problems of wearable biomedical devices.

Photocatalytic BFCs can harvest electrical energy from both light energy and biofuel energy under light induction. For example, a dual-functional silicon nanowire (SiNWs) photocatalyst was synthesized for glucose-based BFCs, in which poly-aniline-functionalized p-type SiNWs and In<sub>2</sub>S<sub>3</sub>-modified n-type SiNWs acted as the cathode and anode.<sup>88</sup> As a result, such a photocatalytic BFC-powered device shows a high open circuit voltage and power density of 0.83 V and 163.01  $\mu\text{W cm}^{-2}$ , respectively (under AM1.5G illumination), which can power the sensor for glucose detection. However, the light-dependent power supplies face the limitations in dark environments, thus limiting their working scenarios. To solve this problem, a bio-sensor powered by an integrated hybrid energy harvesting system consisting of a TENG and an SC has been fabricated for the detection of multiple biomarkers (including Na<sup>+</sup>, K<sup>+</sup>, Ca<sup>2+</sup> and pH).<sup>47</sup> Similarly, a hybrid generator with a TEG and



**Fig. 9** Exemplary works of hybrid systems. (a) Schematic illustration of a hybrid TPENG power supply. Adapted from ref. 85 with permission from the American Chemical Society, Copyright 2024. (b) Schematic illustration of a wearable fabric-based TENG/TEG hybridized energy harvester. Adapted from ref. 87 with permission from Elsevier, Copyright 2022. (c) Schematic illustration of the self-powered supercapacitor as a glucose sensor. Adapted from ref. 93 with permission from Elsevier, Copyright 2024. (d) Schematic illustration of the self-powered supercapacitor by WPT technology. Adapted from ref. 94 with permission from the American Association for the Advancement of Science, Copyright 2023.



an SC has also been incorporated to improve the power output of wearable devices.<sup>89</sup> As a result, wearing this TEG/SC hybrid power supply on the forearm can generate 34 mW h during daytime and 5.9 mW h at night within 30 min. Such dual power supply systems can ensure that wearable biomedical devices remain operational even under low-light conditions or when the user is not in motion, making it a reliable tool for long-term health monitoring.

Supercapacitors (SPCs) are emerging as critical components for energy storage in self-powered systems due to their high-power density, rapid charge/discharge capabilities, and excellent durability. SPCs can store energy by electrostatically accumulating and separating charged ions between the electrolyte and electrode interfaces. By integrating SPCs with TENGs, the energy generated from TENGs can be directly stored without the need for rectifiers or external circuitry. For example, a hybrid SPC/TENG consisted of upper and lower TENGs with a SPC sandwiched between them exhibited excellent self-charging performance.<sup>90</sup> Such a SPC/TENG delivered an energy density of 0.0278 mW h cm<sup>-2</sup> and a power density of 0.089 mW cm<sup>-2</sup>. Similarly, the hybrid SPC/TENG with tissue-like softness has also been successfully applied as an implantable harvester on a porcine heart.<sup>14</sup> Such a stretchable TENG has been attached to a live porcine heart can convert heart beating energy to AC electricity and store it in a stretchable SPC. A pressure-sensitive sensor with an all-yarn-based SPC/TENG as a hybrid power supply can integrate energy harvesting, storage, and sensing together.<sup>91</sup> Besides, glucose sensors integrated with a solid-state supercapacitor and a microneedle-type system also have been developed for continuous glucose monitoring.<sup>92,93</sup> The supercapacitor in the sweat patch can be charged by the glucose-based BFC. Microneedles coated with GOx catalyze the glucose (in sweat) oxidation reaction and generate electrons (Fig. 9c). The glucose concentration in human sweat is proportional to the charging voltage of the supercapacitor. This patch-type BFC-powered glucose sensor not only eliminates the need for an external power supply while remaining light-weight and adaptable to the movements of the human body, ensuring practicality and user comfort.

In addition, supercapacitors can also be charged through WPT technology to supply power in biomedical devices. For example, an implantable drug delivery device was put forward recently, with a Mg receiving coil as the energy harvester and a Zn-ion supercapacitor for energy storage, respectively (Fig. 9d).<sup>94</sup> When the Mg coil receive external electromagnetic waves by WPT technology, the generated AC can be converted into DC power by a small rectifying circuit. After that, the DC output can be used to charge the Zn-ion supercapacitors consisted of anodic zinc foil, cathodic molybdenum sulfide (MoS<sub>2</sub>) nanosheets, and an ion-crosslinked alginate gel electrolyte, which can be safely implanted and gradually degraded within the body over time. Such a self-powered implanted device has been proved to have the ability to power controllable ibuprofen anionic model drug release in a rat model.

## 4. Conclusion and further perspectives

Advanced bioelectronic devices provide a promising approach for biomedical healthcare. In the past few years, a considerable number of emerging self-powered wearable and implantable bioelectronic devices came out with the rapid development of digital healthcare technologies. These devices have integrated various power supplies (*i.e.*, TENGs, PENGs, TEGs, batteries, BFCs and SCs) to enable them operating independently without external power supplies, which opens up new possibilities for diagnostic and therapeutic applications. In this mini-review, the state-of-the-art research progress for recent power supplies in self-powered bioelectronic devices has been discussed, as well as their potential for diagnostic and therapeutic applications. Despite the promising progress of such innovative power supplies in self-powered bioelectronic devices, there is still a long way to go. In this context, our perspectives especially in materials engineering, device design, power management and artificial intelligence are outlined below.

### 4.1. Materials engineering

With the development of materials science, high-performance advanced materials have become essential for the development of power supplies for self-powered biomedical devices. PVDF and its composite materials with good piezoelectric response are widely used in the fabrication of PENG-based devices due to their high biocompatibility and excellent flexibility. Conductive flexible materials including laser-engraved thin metal films, CNTs, conducting polymers, and printable inks allow the fabrication of highly flexible and durable electrodes. Flexible power supplies can be integrated into flexible silicone materials such as PDMS to be worn directly on human skin. In addition, microneedle arrays prepared from various biocompatible materials (*i.e.*, polylactic acid–Au) facilitate the development of mini-invasive therapeutics in drug delivery systems. Some biodegradable materials including metal foils, amino acids and organic polymers are also used in the fabrication of bioresorbable bioelectronic devices. These devices can degrade in the body after a period of operation with no need for surgical extraction. Accordingly, the development of advanced materials will be of great importance toward wireless power supplies in the fabrication of self-powered bioelectronic devices.

### 4.2. Device design

The design of wearable and implantable devices usually demands multiple flexible layers with miniaturized size. However, miniaturization not only means physical size shrinkage, but also put forward requirement for the robustness and consistent power generation capabilities of the devices. Developing flexible or stretchable power supplies with small size is of great importance. For example, the piezoelectric layers (in PENGs), triboelectric layers (in TENGs) and light absorption layers (in SCs) usually demand the thickness of several hundred nanometers, while the thickness of metal foils (in bat-



teries and BFCs) are relatively thicker due to the demand for more power. Technologies that directly use PENG/TENG/battery electrodes as stimulating electrodes can further miniaturize bioelectronic devices, which could potentially allow minimally invasive surgeries for implantable devices.<sup>29,72</sup>

#### 4.3. Power management

The lack of suitable power management will cause considerable energy loss in the self-powered bioelectronic devices. Thus, it is of great necessity to consider the energy efficiency of these power supplies. The use of power management circuits, such as buck converters and boost converters, can minimize energy loss in various self-powered devices through efficient energy storage and power maximization. Generally, the power demand of most miniaturized biomedical devices typically remains at the milliwatt level, which is well within the power output generated by technologies such as TENGs and BFCs. Besides, the suitability of AC (generated from TENGs and PENGs) and DC (generated from TEGs, batteries, BFCs and SCs) should also be considered. A rectifier circuit allows the conversion from AC into DC. In addition, considering the specific operating conditions of different power supplies (*e.g.*, TENGs/PENGs with motion and SCs with sunlight), we believe that hybrid multi-power supplies can ensure a long-term operation under diverse conditions (*e.g.*, low-light conditions or the user not in motion). Accordingly, integrating different types of power supplies is a growing development trend of power management in bioelectronic devices.

#### 4.4. Artificial intelligence

The development of artificial intelligence technologies has also promoted the medical diagnostics and therapeutics of bioelectronic devices. Although the application of artificial intelligence in bioelectronic devices is still in infancy, some researchers have already combined machine learning (*e.g.*, deep learning neural networks) with sweat sensor patches to improve their accuracy, usability, and convenience for disease diagnosis.<sup>95</sup> We could anticipate increased integration of artificial intelligence technologies into smart self-powered bioelectronic devices in the future, including machine learning, computer vision, *etc.*

### Author contributions

Y. X., B. S., and Y. Z. wrote the draft of the manuscript, organized the figures, and selected the appropriate references. Y. K., B. Z., J. C. and K. S. helped to revise the manuscript. Y. Z. conceived the theme and the outline of this manuscript and directed the research program.

### Data availability

No primary research results, software or code have been included and no new data were generated or analysed as part of this mini-review.

### Conflicts of interest

There are no conflicts to declare.

### Acknowledgements

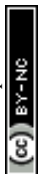
The authors acknowledge support from the National University of Singapore start-up grant. Yu Xin would like to acknowledge the support provided by the China Scholarship Council (CSC) during his research visit to Singapore (No. 202306150046). Jiayang Chen thanks the undergraduate overseas scientific research internship support program from the College of Chemistry, Nankai University, China.

### References

- 1 T. Jiang, B.-F. Zeng, B. Zhang and L. Tang, *Chem. Soc. Rev.*, 2023, **52**, 5968–6002.
- 2 R. Kaveti, M. A. Jakus, H. Chen, B. Jain, D. G. Kennedy, E. A. Caso, N. Mishra, N. Sharma, B. E. Uzunoğlu, W. B. Han, T.-M. Jang, S.-W. Hwang, G. Theocharidis, B. J. Sumpio, A. Veves, S. K. Sia and A. J. Bhandodkar, *Sci. Adv.*, 2024, **10**, eado7538.
- 3 Y. Lyu, H. Huang, Y. Su, B. Ying, W.-C. Liu, K. Dong, N. Du, R. S. Langer, Z. Gu and K. Nan, *Matter*, 2024, **7**, 1440–1465.
- 4 J. Wu, H. Liu, W. Chen, B. Ma and H. Ju, *Nat. Rev. Bioeng.*, 2023, **1**, 346–360.
- 5 E. Chatzilakou, Y. Hu, N. Jiang and A. K. Yetisen, *Biosens. Bioelectron.*, 2024, **250**, 116045.
- 6 K. Sankar, U. Kuzmanović, S. E. Schaus, J. E. Galagan and M. W. Grinstaff, *ACS Sens.*, 2024, **9**, 2254–2274.
- 7 M. A. Beach, U. Nayanathara, Y. Gao, C. Zhang, Y. Xiong, Y. Wang and G. K. Such, *Chem. Rev.*, 2024, **124**, 5505–5616.
- 8 B. Hu, D. Xu, Y. Shao, Z. Nie, P. Liu, J. Li, L. Zhou, P. Wang, N. Huang, J. Liu, Y. Lu, Z. Wu, B. Wang, Y. Mei, M. Han, R. Li and E. Song, *Sci. Adv.*, 2024, **10**, eadp8804.
- 9 H. Zhang, Y. Pan, Y. Hou, M. Li, J. Deng, B. Wang and S. Hao, *Small*, 2023, **20**, 2306944.
- 10 B. Luo, Q. Zhou, W. Chen, L. Sun, L. Yang, Y. Guo, H. Liu, Z. Wu, R. E. Neisiany, X. Qin, J. Pan and Z. You, *Nano Lett.*, 2023, **23**, 2927–2937.
- 11 H. Xue, J. Jin, Z. Tan, K. Chen, G. Lu, Y. Zeng, X. Hu, X. Peng, L. Jiang and J. Wu, *Sci. Adv.*, 2024, **10**, eadn0260.
- 12 S. Wang, Q. Cui, P. Abiri, M. Roustaei, E. Zhu, Y.-R. Li, K. Wang, S. Duarte, L. Yang, R. Ebrahimi, M. Bersohn, J. Chen and T. K. Hsiai, *Sci. Adv.*, 2023, **9**, eadj0540.
- 13 H. Kang, W. B. Han, S. M. Yang, G.-J. Ko, Y. Ryu, J. H. Lee, J.-W. Shin, T.-M. Jang, K. Rajaram, S. Han, D.-J. Kim, J. H. Lim, C.-H. Eom, A. J. Bhandodkar and S.-W. Hwang, *Chem. Eng. J.*, 2023, **475**, 146208.
- 14 P. Cheng, S. Dai, Y. Liu, Y. Li, H. Hayashi, R. Papani, Q. Su, N. Li, Y. Dai, W. Liu, H. Hu, Z. Liu, L. Jin, N. Hibino, Z. Wen, X. Sun and S. Wang, *Device*, 2024, **2**, 100216.



- 15 Y. Hu, Y. Wang, F. Yang, D. Liu, G. Lu, S. Li, Z. Wei, X. Shen, Z. Jiang, Y. Zhao, Q. Pang, B. Song, Z. Shi, S. Shafique, K. Zhou, X. Chen, W. Su, J. Jian, K. Tang, T. Liu and Y. Zhu, *Adv. Sci.*, 2024, **11**, 2307746.
- 16 H. Dinis and P. M. Mendes, *Biosens. Bioelectron.*, 2021, **172**, 112781.
- 17 J. He, L. Cao, J. Cui, G. Fu, R. Jiang, X. Xu and C. Guan, *Adv. Mater.*, 2024, **36**, 2306090.
- 18 W. Tang, Q. Sun and Z. L. Wang, *Chem. Rev.*, 2023, **123**, 12105–12134.
- 19 Q. Zheng, Q. Tang, Z. L. Wang and Z. Li, *Nat. Rev. Cardiol.*, 2021, **18**, 7–21.
- 20 S. Zhang, X. Lin, J. Wan, C. Xu and M. Han, *Adv. Mater. Technol.*, 2024, **9**, 2301895.
- 21 T. Cheng, J. Shao and Z. L. Wang, *Nat. Rev. Methods Primers*, 2023, **3**, 39.
- 22 X. Tao, X. Chen and Z. L. Wang, *Energy Environ. Sci.*, 2023, **16**, 3654–3678.
- 23 C. Xu, J. Yu, Z. Huo, Y. Wang, Q. Sun and Z. L. Wang, *Energy Environ. Sci.*, 2023, **16**, 983–1006.
- 24 W. Deng, Y. Zhou, A. Libanori, G. Chen, W. Yang and J. Chen, *Chem. Soc. Rev.*, 2022, **51**, 3380–3435.
- 25 S. Bairagi, S. Islam, M. Shahadat, D. M. Mulvihill and W. Ali, *Nano Energy*, 2023, **111**, 108414.
- 26 M. H. Bagheri, A. A. Khan, S. Shahzadi, M. M. Rana, M. S. Hasan and D. Ban, *Nano Energy*, 2024, **120**, 109101.
- 27 J. He, K. Li, L. Jia, Y. Zhu, H. Zhang and J. Linghu, *Appl. Therm. Eng.*, 2024, **236**, 121813.
- 28 S. Hwang, D. Jang, B. Lee, Y. Ryu, J. Kwak, H. Kim and S. Chung, *Adv. Energy Mater.*, 2023, **13**, 2204171.
- 29 Y. Zhang, F. Liu, Y. Zhang, J. Wang, D. D'Andrea, J. B. Walters, S. Li, H.-J. Yoon, M. Wu, S. Li, Z. Hu, T. Wang, J. Choi, K. Bailey, E. Dempsey, K. Zhao, A. Lantsova, Y. Bouricha, I. Huang, H. Guo, X. Ni, Y. Wu, G. Lee, F. Jiang, Y. Huang, C. K. Franz and J. A. Rogers, *Proc. Natl. Acad. Sci. U. S. A.*, 2023, **120**, e2217734120.
- 30 H. Wu, Y. Wang, H. Li, Y. Hu, Y. Liu, X. Jiang, H. Sun, F. Liu, A. Xiao, T. Chang, L. Lin, K. Yang, Z. Wang, Z. Dong, Y. Li, S. Dong, S. Wang, J. Chen, Y. Liu, D. Yin, H. Zhang, M. Liu, S. Kong, Z. Yang, X. Yu, Y. Wang, Y. Fan, L. Wang, C. Yu and L. Chang, *Nat. Electron.*, 2024, **7**, 299–312.
- 31 N. T. Garland, R. Kaveti and A. J. Bandodkar, *Adv. Mater.*, 2023, **35**, 2303197.
- 32 X. Xiao, *eScience*, 2022, **2**, 1–9.
- 33 J. L. Zhang, Y. H. Wang, K. Huang, K. J. Huang, H. Jiang and X. M. Wang, *Nano Energy*, 2021, **84**, 105853.
- 34 S. ul Haque, A. Nasar, N. Duteanu, S. Pandey and Inamuddin, *Fuel*, 2023, **331**, 125634.
- 35 L. Yin, J.-M. Moon, J. R. Sempionatto, M. Lin, M. Cao, A. Trifonov, F. Zhang, Z. Lou, J.-M. Jeong, S.-J. Lee, S. Xu and J. Wang, *Joule*, 2021, **5**, 1888–1904.
- 36 J. Min, S. Demchyshyn, J. R. Sempionatto, Y. Song, B. Hailegnaw, C. Xu, Y. Yang, S. Solomon, C. Putz, L. E. Lehner, J. F. Schwarz, C. Schwarzinger, M. C. Scharber, E. Shirzaei Sani, M. Kaltenbrunner and W. Gao, *Nat. Electron.*, 2023, **6**, 630–641.
- 37 Y. S. Choi, H. Jeong, R. T. Yin, R. Avila, A. Pfenniger, J. Yoo, J. Y. Lee, A. Tzavelis, Y. J. Lee, S. W. Chen, H. S. Knight, S. Kim, H.-Y. Ahn, G. Wickerson, A. Vázquez-Guardado, E. Higbee-Dempsey, B. A. Russo, M. A. Napolitano, T. J. Holleran, L. A. Razzak, A. N. Miniovich, G. Lee, B. Geist, B. Kim, S. Han, J. A. Brennan, K. Aras, S. S. Kwak, J. Kim, E. A. Waters, X. Yang, A. Burrell, K. San Chun, C. Liu, C. Wu, A. Y. Rwei, A. N. Spann, A. Banks, D. Johnson, Z. J. Zhang, C. R. Haney, S. H. Jin, A. V. Sahakian, Y. Huang, G. D. Trachiotis, B. P. Knight, R. K. Arora, I. R. Efimov and J. A. Rogers, *Science*, 2022, **376**, 1006–1012.
- 38 J. Kim, J. Jeon, J. Lee, B. Khoroldulam, S. Choi, J. Bae, J. K. Hyun and S. Kang, *Adv. Sci.*, 2023, **10**, 2302632.
- 39 S. Wang, Q. Cui, P. Abiri, M. Roustaei, E. Zhu, Y.-R. Li, K. Wang, S. Duarte, L. Yang, R. Ebrahimi, M. Bersohn, J. Chen and T. K. Hsiai, *Sci. Adv.*, 2023, **9**, eadj0540.
- 40 R. Liu, Z. L. Wang, K. Fukuda and T. Someya, *Nat. Rev. Mater.*, 2022, **7**, 870–886.
- 41 A. Khan, R. Joshi, M. K. Sharma, A. Ganguly, P. Parashar, T.-W. Wang, S. Lee, F.-C. Kao and Z.-H. Lin, *Nano Energy*, 2024, **119**, 109051.
- 42 Y. Wang, J. Zhang, X. Jia, M. Chen, H. Wang, G. Ji, H. Zhou, Z. Fang and Z. Gao, *Nano Energy*, 2024, **119**, 109080.
- 43 X. Xiao, X. Xiao, A. Nashalian, A. Libanori, Y. Fang, X. Li and J. Chen, *Adv. Healthc. Mater.*, 2021, **10**, 2100975.
- 44 Z. Liu, Y. Hu, X. Qu, Y. Liu, S. Cheng, Z. Zhang, Y. Shan, R. Luo, S. Weng, H. Li, H. Niu, M. Gu, Y. Yao, B. Shi, N. Wang, W. Hua, Z. Li and Z. L. Wang, *Nat. Commun.*, 2024, **15**, 507.
- 45 Y. Liao, S. Tian, Y. Li, L. Li, X. Chen, J. Chen, F. Yang and M. Gao, *Nano Energy*, 2024, **128**, 109915.
- 46 X. Yuan, P. Qiu, C. Sun, S. Yang, Y. Wu, L. Chen and X. Shi, *Energy Environ. Sci.*, 2024, **17**, 4968–4976.
- 47 R. Omar, M. Yuan, J. Wang, M. Sublaban, W. Saliba, Y. Zheng and H. Haick, *Sens. Actuators, B*, 2024, **398**, 134788.
- 48 Y. Liu, S. Yue, Z. Tian, Z. Zhu, Y. Li, X. Chen, Z. L. Wang, Z. Yu and D. Yang, *Adv. Mater.*, 2024, **36**, 2309893.
- 49 Z. Lai, J. Xu, C. R. Bowen and S. Zhou, *Joule*, 2022, **6**, 1501–1565.
- 50 Y. Yang, L. Xu, D. Jiang, B. Z. Chen, R. Luo, Z. Liu, X. Qu, C. Wang, Y. Shan, Y. Cui, H. Zheng, Z. Wang, Z. L. Wang, X. D. Guo and Z. Li, *Adv. Funct. Mater.*, 2021, **31**, 2104092.
- 51 Y. Chen, X. Wan, G. Li, J. Ye, J. Gao and D. Wen, *Adv. Funct. Mater.*, 2024, **34**, 2404329.
- 52 Y. Zhang, B. Ge, J. Feng, N. Kuang, H. Ye, Z. Yuan, M. Wu, B. Jiang, J. Li, Q. Sun, L. Niu, M. Zhu, Y. Xu, W. Jie, R. Liu, S. Dong and C. Zhou, *Adv. Funct. Mater.*, 2024, **34**, 2403990.
- 53 K. Shi, B. Chai, H. Zou, Z. Wen, M. He, J. Chen, P. Jiang and X. Huang, *Adv. Funct. Mater.*, 2023, **33**, 2307678.
- 54 A. Chen, Q. Zeng, L. Tan, F. Xu, T. Wang, X. Zhang, Y. Luo and X. Wang, *Energy Environ. Sci.*, 2023, **16**, 3486–3496.
- 55 S. Zhang, T. Jiang, F. Han, L. Cao, M. Li, Z. Ge, H. Sun, H. Wu, W. Wu, N. Zhou, M. L. Akhtar and H. Jiang, *Chem. Eng. J.*, 2024, **480**, 148347.



- 56 C. Wang, G. He, H. Zhao, Y. Lu, P. Jiang and W. Li, *Adv. Mater.*, 2024, **36**, 2311246.
- 57 W. Harmon, D. Bamgboje, H. Guo, T. Hu and Z. L. Wang, *Nano Energy*, 2020, **71**, 104642.
- 58 L. Qian, F. Jin, Z. Wei, T. Li, Z. Sun, C. Lai, J. Ma, R. Xiong, X. Ma, F. Wang, F. Sun, W. Zheng, W. Dong, K. Sun, T. Wang and Z. Feng, *Adv. Funct. Mater.*, 2023, **33**, 2209407.
- 59 W. Zhang, X. Qin, G. Li, X. Zhou, H. Li, D. Wu, Y. Song, K. Zhao, K. Wang, X. Feng, L. Tan, B. Wang, X. Sun, Z. Wen and C. Yang, *Nat. Commun.*, 2024, **15**, 5736.
- 60 Y. Yang, R. Luo, S. Chao, J. Xue, D. Jiang, Y. H. Feng, X. D. Guo, D. Luo, J. Zhang, Z. Li and Z. L. Wang, *Nat. Commun.*, 2022, **13**, 6908.
- 61 Y. Wu, K. Zhang, S. Li, Z. Xiang, G. Jiang, R. Zhang, Y. Qi, X. Ji, X. Cai, C. Zhang, J. Li, R. Yan, H. Jin, S. Dong, J. Luo and G. Feng, *Nano Energy*, 2024, **121**, 109234.
- 62 G. Yao, L. Kang, C. Li, S. Chen, Q. Wang, J. Yang, Y. Long, J. Li, K. Zhao, W. Xu, W. Cai, Y. Lin and X. Wang, *Proc. Natl. Acad. Sci. U. S. A.*, 2021, **118**, e2100772118.
- 63 R. Qiu, X. Zhang, C. Song, K. Xu, H. Nong, Y. Li, X. Xing, K. Mequanint, Q. Liu, Q. Yuan, X. Sun, M. Xing and L. Wang, *Nat. Commun.*, 2024, **15**, 4133.
- 64 D.-M. Lee, M. Kang, I. Hyun, B.-J. Park, H. J. Kim, S. H. Nam, H.-J. Yoon, H. Ryu, H. Park, B.-O. Choi and S.-W. Kim, *Nat. Commun.*, 2023, **14**, 7315.
- 65 Y. Zhang, L. Xu, Z. Liu, X. Cui, Z. Xiang, J. Bai, D. Jiang, J. Xue, C. Wang, Y. Lin, Z. Li, Y. Shan, Y. Yang, L. Bo, Z. Li and X. Zhou, *Nano Energy*, 2021, **85**, 106009.
- 66 Z. Chen, Y. Lai, S. Xu, M. Zhu, Y. Sun, Y. Cheng and G. Zhao, *Nano Energy*, 2024, **123**, 109344.
- 67 S. Liang, H. Guan, G. Yang, W. Lin, Z. Long, T. Zhong, R. Lin, L. Xing, Y. Zhang, G. Li, M. Chen, X. Xue and Y. Zhan, *Nano Energy*, 2023, **115**, 108764.
- 68 L. Jiang, L. Zhang, C. Dai, B. Zhao, Y. Yang, Z. Wu, C. Qu, L. Zou, Z.-H. Lin, Y.-B. Miao and Y. Shi, *Nano Energy*, 2024, **119**, 109040.
- 69 X.-L. Shi, L. Wang, W. Lyu, T. Cao, W. Chen, B. Hu and Z.-G. Chen, *Chem. Soc. Rev.*, 2024, **53**, 9254–9305.
- 70 Y. Zheng, X. Han, J. Yang, Y. Jing, X. Chen, Q. Li, T. Zhang, G. Li, H. Zhu, H. Zhao, G. J. Snyder and K. Zhang, *Energy Environ. Sci.*, 2022, **15**, 2374–2385.
- 71 I. Huang, Y. Zhang, H. M. Arafa, S. Li, A. Vazquez-Guardado, W. Ouyang, F. Liu, S. Madhvapathy, J. W. Song, A. Tzavelis, J. Trueb, Y. Choi, W. J. Jeang, V. Forsberg, E. Higbee-Dempsey, N. Ghoreishi-Haack, I. Stepien, K. Bailey, S. Han, Z. J. Zhang, C. Good, Y. Huang, A. J. Bandodkar and J. A. Rogers, *Energy Environ. Sci.*, 2022, **15**, 4095–4108.
- 72 Y. Zhou, X. Jia, D. Pang, S. Jiang, M. Zhu, G. Lu, Y. Tian, C. Wang, D. Chao and G. Wallace, *Nat. Commun.*, 2023, **14**, 297.
- 73 L. Wang, C. Lu, S. Yang, P. Sun, Y. Wang, Y. Guan, S. Liu, D. Cheng, H. Meng, Q. Wang, J. He, H. Hou, H. Li, W. Lu, Y. Zhao, J. Wang, Y. Zhu, Y. Li, D. Luo, T. Li, H. Chen, S. Wang, X. Sheng, W. Xiong, X. Wang, J. Peng and L. Yin, *Sci. Adv.*, 2020, **6**, eabc6686.
- 74 S. Li, Y. Cheng, K. Deng and H. Sun, *Nano Energy*, 2024, **124**, 109461.
- 75 A. J. Bandodkar, S. P. Lee, I. Huang, W. Li, S. Wang, C.-J. Su, W. J. Jeang, T. Hang, S. Mehta, N. Nyberg, P. Gutruf, J. Choi, J. Koo, J. T. Reeder, R. Tseng, R. Ghaffari and J. A. Rogers, *Nat. Electron.*, 2020, **3**, 554–562.
- 76 E. De la Paz, N. H. Maganti, A. Trifonov, I. Jeerapan, K. Mahato, L. Yin, T. Sonsa-ard, N. Ma, W. Jung, R. Burns, A. Zarrinpar, J. Wang and P. P. Mercier, *Nat. Commun.*, 2022, **13**, 7405.
- 77 Y. Guo, C. Chen, J. Feng, L. Wang, J. Wang, C. Tang, X. Sun and H. Peng, *Small Methods*, 2022, **6**, 2200142.
- 78 M. Yan, Z. Wu, Z. Li, Z. Li, J. Wang and Z. Hu, *Biosens. Bioelectron.*, 2024, **259**, 116365.
- 79 Y. Yu, J. Nassar, C. Xu, J. Min, Y. Yang, A. Dai, R. Doshi, A. Huang, Y. Song, R. Gehlhar, A. D. Ames and W. Gao, *Sci. Rob.*, 2020, **5**, eaaz7946.
- 80 M. Sun, Y. Gu, X. Pei, J. Wang, J. Liu, C. Ma, J. Bai and M. Zhou, *Nano Energy*, 2021, **86**, 106061.
- 81 M. Mohammadifar, M. Tahernia, J. H. Yang, A. Koh and S. Choi, *Nano Energy*, 2020, **75**, 104994.
- 82 J. Ryu, M. Landers and S. Choi, *Biosens. Bioelectron.*, 2022, **205**, 114128.
- 83 H. Jinno, T. Yokota, M. Koizumi, W. Yukita, M. Saito, I. Osaka, K. Fukuda and T. Someya, *Nat. Commun.*, 2021, **12**, 2234.
- 84 Y. Li, Z. Chen, Y. Liu, Z. Liu, T. Wu, Y. Zhang, L. Peng, X. Huang, S. Huang, X. Lin, X. Xie and L. Jiang, *Natl. Sci. Rev.*, 2024, **11**, nwae062.
- 85 A. Huang, Y. Zhu, S. Peng, B. Tan and X. Peng, *ACS Nano*, 2024, **18**, 691–702.
- 86 Q. Chen, Y. Cao, Y. Lu, W. Akram, S. Ren, L. Niu, Z. Sun and J. Fang, *ACS Appl. Mater. Interfaces*, 2024, **16**, 6239–6249.
- 87 W.-G. Kim, D. Kim, H. M. Lee and Y.-K. Choi, *Nano Energy*, 2022, **100**, 107485.
- 88 H.-J. Li, C. Chen, X. Zhang, C. Huang, Z. Chen, T. Wang, D. Wang, L. Xu and J. Fan, *J. Power Sources*, 2024, **603**, 234432.
- 89 Y. J. Kim, S. E. Park and B. J. Cho, *Nano Energy*, 2022, **93**, 106775.
- 90 K. Shrestha, S. Sharma, G. B. Pradhan, T. Bhatta, S. S. Rana, S. Lee, S. Seonu, Y. Shin and J. Y. Park, *Nano Energy*, 2022, **102**, 107713.
- 91 R. Tao, Y. Mao, C. Gu and W. Hu, *Chem. Eng. J.*, 2024, **496**, 154358.
- 92 H.-J. Kil, S.-R. Kim and J.-W. Park, *ACS Appl. Mater. Interfaces*, 2022, **14**, 3838–3848.
- 93 H.-J. Kil, J. H. Kim, K. Lee, T.-U. Kang, J.-H. Yoo, Y. Lee and J.-W. Park, *Biosens. Bioelectron.*, 2024, **257**, 116297.
- 94 H. Sheng, L. Jiang, Q. Wang, Z. Zhang, Y. Lv, H. Ma, H. Bi, J. Yuan, M. Shao, F. Li, W. Li, E. Xie, Y. Liu, Z. Xie, J. Wang, C. Yu and W. Lan, *Sci. Adv.*, 2023, **15**, eadh8083.
- 95 X. T. Zheng, Z. Yang, L. Sutarlie, M. Thangaveloo, Y. Yu, N. A. B. M. Salleh, J. S. Chin, Z. Xiong, D. L. Becker, X. J. Loh, B. C. K. Tee and X. Su, *Sci. Adv.*, 2023, **9**, eadg6670.

